IOSR Journal of Mechanical and Civil Engineering (IOSR-JMCE)
e-ISSN: 2278-1684,p-ISSN: 2320-334X, Volume 17, Issue 2 Ser. V (Mar - Apr 2020), PP 35-43
www.iosrjournals.org

Finite Element Modeling of Lightweight Concrete Slabs with Expanded Metal Mesh

Hany A. Dahish[1,2] and Ahmed M. EL-Kholy[1]
[1]*Civil Engineering Department, Faculty of Engineering, Fayoum University, Egypt*
[2]*Civil Engineering Department, College of Engineering, Qassim University, Saudi Arabia*
Corresponding Author: Hany A. Dahish

Abstract:
In this paper, numerical simulations of the punching shear failure of reinforced concrete slabs with light weight aggregates and concrete slabs reinforced with expanded metal mesh have been made. The importance of the studying of the punching shear failure was due to its brittle and sudden failure. The numerical models of punching shear failure for these types of slabs were made by the utilization of finite element analysis software (ANSYS V.2020.R1). The nonlinear behavior of concrete and steel were taken into consideration in these models. The used elements in modeled slabs were solid element to model concrete, space bar element to model the reinforcement and the embedded smeared layer within the solid element to model the expanded metal mesh. All used experimental data in this paper were obtained from literature. The results of numerical models of the slabs were compared with the experimental results from literature by means ofultimate loads, crack patterns and load-deflection responses. Good agreement of the numerical models results with experimental results were obtained. The numerical models of this study can be used as tools to predict the punching shear capacity of concrete slab with light weight aggregate and concrete slabs reinforced with expanded metal mesh.
Key Word*:Punching shear; Nonlinear FEA; Ferrocement; Lightweight concrete; Concrete slab*

Date of Submission: 11-04-2020 Date of Acceptance: 26-04-2020

I. Introduction

The punching shear failure of reinforced concrete flat slab is considered one of the important design issues in the design of reinforced concrete slabs subjected to concentrated loads or around the supported columns as a result of the sudden brittle failure. The experimental investigations of the behavior of normal and lightweight reinforced concrete slabs, and also concrete slabs reinforced with Expanded Metal Mesh (EMM) layer had been conducted by many researchers.

The light weight aggregate concrete (LWAC) is a versatile material due to its high strength to weight ratio. An experimental work had been conducted to study the punching shear behavior of LWAC slabs using two different types of light weight aggregatesand it was concluded that the type of lightweight aggregate affects the surface failure angle of punching shear (Youm et al., 2014). The reduction factors for punching shear strength of five light weight reinforced concrete slabs were investigated and it was concluded that the punching shear strength decreased as the density of aggregate decreased (Higashiyama et al., 2010).

An experimental study on three slab column connections of 7620 mm in length as a flat slab structure to evaluate the effectiveness of stud rails that placed in an orthogonal or radial layouts in slab–column connections whose slabs have relatively low flexural reinforcement ratios had been conducted and it was concluded that the placement of stud rails in radial layout was better than that in orthogonal layout in increasing the shear strength of slab–column connections because it provides ductile post-flexural yielding behavior (Thai et al., 2016).

An attempt was made to study the behavior of light weight silica fume aggregate concrete at elevated temperature (Venkateswarluet al., 2018). The authors showed that the increase in the replacement level of aggregate with silica fume aggregate increased the workability and decreasedboth density and compressive strength.The use of pre-wetted light weight aggregates that allow concrete to use the water for cement hydration as per need as a new technique for internal curing was investigated andit was concluded that it improved the hydration and reducedboth cracking and shrinkage of concrete (Tamboli et al., 2016).

Ferrocement is used as low cost structural element. It is a composite thin construction material that constructed by cementitious mortar with layers of expanded wire mesh (Naamanet al., 2016). Ferrocement was used in many concrete structures as water tanks, silos and it can be used as repair material because it needs no advanced techniques during installation.

Ferrocement might be considered as the best alternative to concrete and steel (Ibrahim, 2011). Ibrahim, (2011) tested a twenty-seven simply supported square cementitious slabs with dimensions of 490x490x40 mm to 490x490x60 mm under the effect of patch loading. The test parameters were the volume fraction of the wire mesh (0.12 to 1.41), the slab thickness (40 to 60 mm), the patch load pattern (square or rectangle) and the type of wire mesh (Welded Wire Mesh or Expanded Metal Mesh). The ultimate capacities wereinvestigated for both cementitious slabs with ferrocement layers and for slabs with reinforcement grids.It was concluded that the increase in the volume fraction of wire mesh increased the punching shear resistance of the slab and the addition of Expanded Metal Mesh to regular reinforcement grid increased the punching shear strength at column stub.

A back-propagation neural network (BPNN) model to predict the punching shear strength of square ferrocement slabs based on data collected from different sources had been developed (Mashrei, 2012).An experimental work had been conducted by testing a thirty-one simply supported square ferrocement slabs subjected to central concentrated loading (Mansuret al., 2001).They concluded that critical punching shear perimeter might be located at a distance from the edge of the loading plateequals one and half times the thickness of the slab. The punching shear strength of ferrocement slabs had been experimentally investigated (Paramasivamet al., 1993).

Numerical models provide sound alternative and became a useful tool for experimental investigations. The utilization of large purpose computer codes is acceptable for the analysis of various types of structures. These codes can be used to simulate the deformations and stresses of very complex structures with acceptable accuracy.

In the present study, the punching shear failure of normal, light weight reinforced concrete slabs and cementitious slabs reinforced with Expanded Metal Mesh were numerically modeled utilizing nonlinear finite element analysis (FEA). The numerical results were compared with experimental results obtained from literature [(Youm et al., 2014) and (Ibrahim, 2011)]. The present study will be extended in a further paper to include other parameters affected the punching shear strength of different types of concrete slabs.

II. Material Properties

The material properties of the modeled slabs form literature areshown in Table no 1, the table includes group ID, slab thickness, mechanical properties of used concrete as compressivestrength, tensile strength and modulus of elasticity in addition to the volume fraction of the wire mesh.

Table no 1: Material properties of modeled concrete and cementitious slabs

Group	Specimen	Thickness mm	Compressive strength f_c' (MPa)	Tensile strength f_{sp} (MPa)	Modulus of Elasticity E_c (GPa)	Volume fraction v_f	Reference
1	NN	200	40.6	3.41	31.7	---	Youm et al. (2014)
	LA	200	37.2	3.40	22.6	---	
	LD	200	34.2	2.82	20.0	---	
2	Slab-I	40	32.0	5.20	24.9	---	Ibrahim, (2011)
	Slab-Ø6	50	32.0	5.20	24.9	1.41	
	DP-2.0	50	32.0	5.20	24.9	0.60	

Table no 2 shows the material properties of used steel bars. Bars of 10 mm in diameterwere used in group1 and bars of 6 mm in diameterwere used in Slab-Ø6 specimen in group 2.

Table no 2: Material properties of usedsteel bars

	Ø10 mm steel bars	Ø6 mm steel bars
Yield stress	411 MPa	252 MPa
Ultimate strength	600 MPa	364 MPa
Elongation	12 %	30 %
Elastic modulus	200 GPa	195 GPa

Table no 3 shows the material properties of the Expanded Metal Mesh (EMM) that utilized in DP-2.0 specimen in group 2.

Table no 3: Material properties of (EMM)

Diamond size	22.5x57.5 mm
Dimension of strand	2 mm
Proof stress	300 MPa
Proof strain	0.117%
Ultimate strength	500 MPa
Ultimate strain	5.4%

III. Details of Simulated Concrete Slabs

The first group (Youm et al., 2014)consisted of one normalweight concrete slab (NN) and two lightweight concrete slabs (LA and LD). All the three slabs had same dimensions and reinforcement layout. Figure no 1shows the dimensions of slabs and the layout of reinforcement of the first group.The top and bottom cover depths were 20 mm. The vertical displacement was applied through 300 mm square steel plates with thickness of 35 mm.

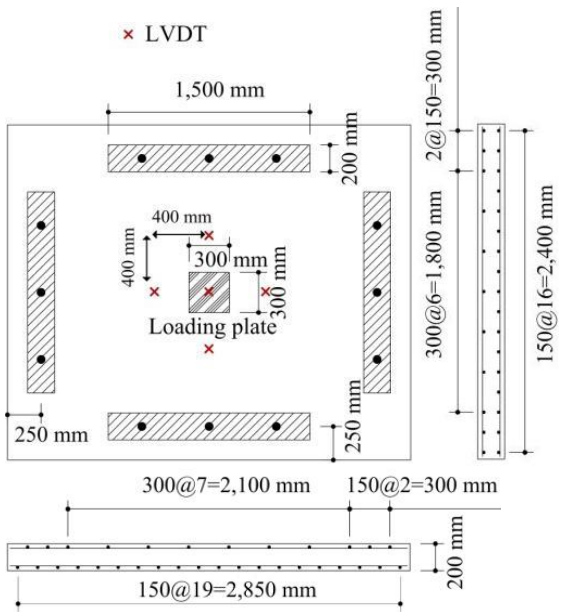

Figure no 1: NN, LA and LD specimens(Youm et al., 2014)

The second group consisted of twenty-seven square cementitious slabs of 490x490mm with thickness of 40, 45, 50 and 60 mm (Ibrahim, 2011). The slabs were supported on its four edges. The clear span of the slabs was 400x400 mm. The slabs were subjected to patch load pattern (square or rectangle). In the present study, three specimens (Slab-I, Slab-Ø6 and DP-2.0) were modeled. The first slab was a plain mortar slab. The second slab was a cementitious slab reinforced with 6 mm steel bars arranged in two orthogonal directions and spaced 100 mm apart. The third specimen is a cementitious slab reinforced with ferrocement layer of EMM with strand thickness of 2 mm. The vertical displacement was applied through 80 mm square steel plate with thickness of 20 mm. Figure no 2 shows the dimensions and reinforcement layouts of the slabs.

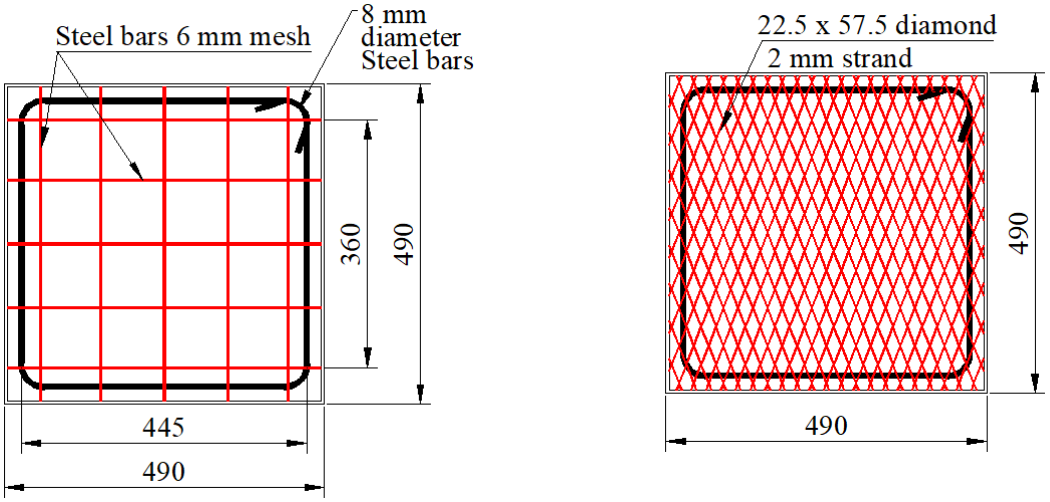

(a) Slab-Ø6 (b) DP-2.0

Figure no 2: Specimens dimensions and reinforcement details of the slabs (Ibrahim, 2011)

IV. Finite Element Model

The developed FE models were based on the experimental plans (Youm et al., 2014) and (Ibrahim, 2011). The following steps describes the process of the proposed finite element models.

Concrete, ferrocement layer and reinforcement grid

All slabs were modeled utilizing finite element analysis software (ANSYS V.2020.R1) [11],which offers robust nonlinear analysis capabilities. Routines were written in ANSYS to model the six specimens (NN, LA, LD, Slab-I, Slab-Ø6 and DP-2.0).The concrete element adopted in presented finite element model was Solid65. Solid 65 is a three dimensional solid element as shown in figure no 3 and has eight nodes with three degrees of freedom at each node (translations in x, y, and z directions). The element is capable of cracking in tension, crushing in compression, modeling the creep and simulating both material and geometrical nonlinearities. EMM layer was simulated as smeared layer embedded within the solid elements(Taha et al., 2018). Two shear transfer coefficients, one for open cracks (0.3) and other for closed ones (0.6), were set to model the shear transfer in cracked concrete elements(Khan et al., 2014).

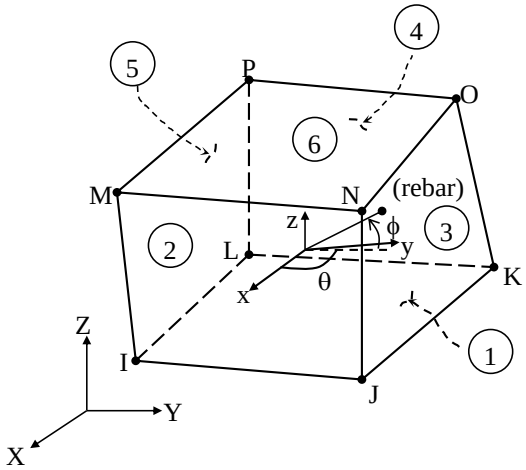

Figure no 3: Geometry, node locations and coordinate system of Solid65 element

Link8 element was used to model the reinforcement grid for specimens without ferrocement layer as shown in figure no 4. Link8 is a space bar element subjected to uniaxial force with three degrees of freedom (translations in x, y, and z directions) at each node. Link8 simulates material nonlinearity and large deformation behavior.

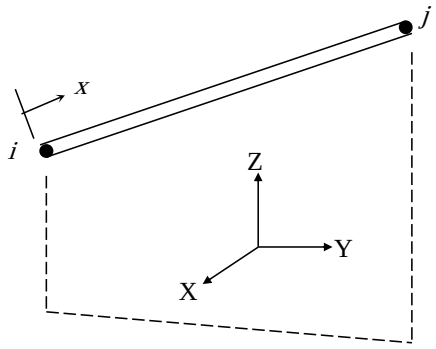

Figure no 4: Geometry, node locations and coordinate system of Link8 element

Figure no 5 shows the modelofreinforcement bars whereas figure no6 shows the concrete meshutilizing solid elements.

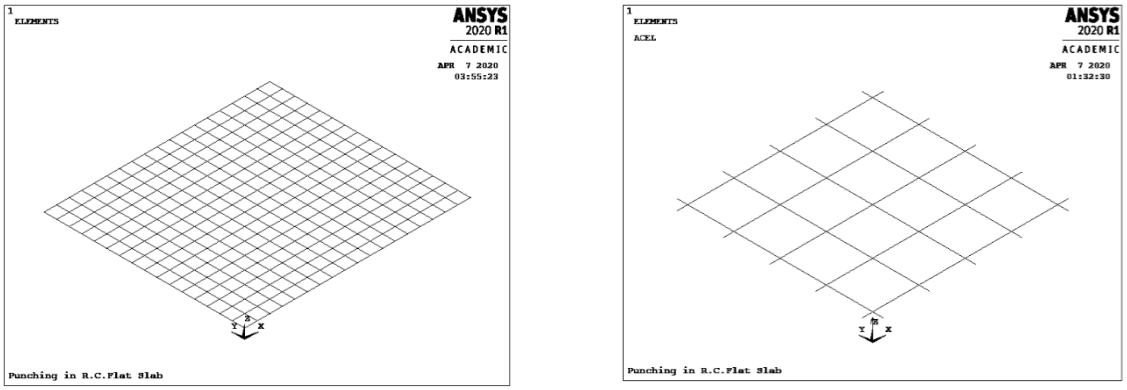

Figure no 5: Meshed elements (link8) for modeling of reinforcement grid

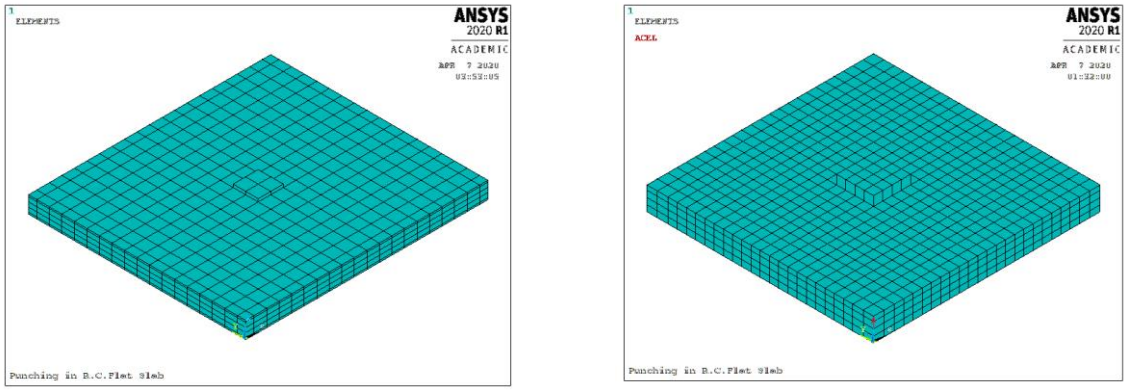

Figure no 6: Meshed elements (solid65) for modeling of concrete and cementitious slabs

Material properties modeling and plastic deformation

Figure no 7 show the stress-strain curve for Ø 10 mm steel bars used as reinforcement forspecimens of group 1.Figure no 8 shows the stress-strain curve for concrete for LA specimen. Poisson's ratios were set as 0.2 and 0.3 for concrete and steel, respectively.

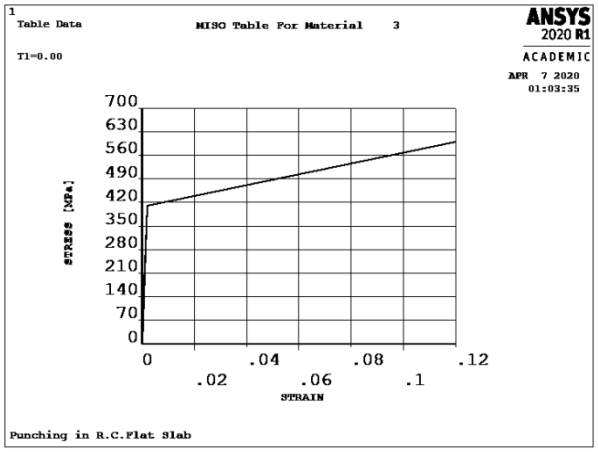

Figure no 7: Stress-strain curve for steel bars 10 mm

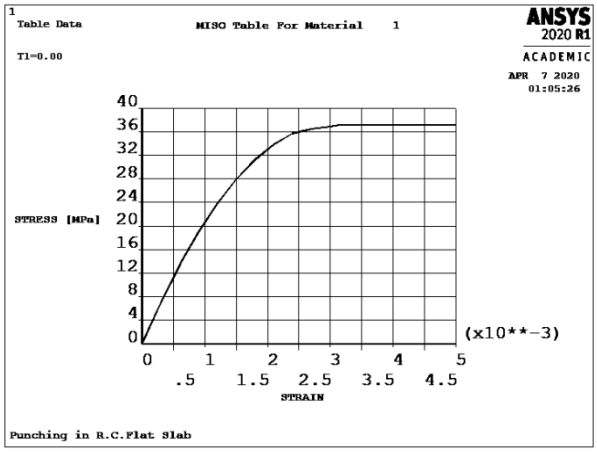

Figure no 8: Stress-strain curve for utilized concrete

Loading and boundary conditions

The boundary conditions (restrained translations in x, y and z directions) were set at four edges of slabs to simulate the simply supported conditions similar to experimental work. For top surface of loading plate, vertical displacement has been applied in fine increments in negative Z-direction for all joints to represent the actual loading procedure. Figure no 9 shows the boundary conditions at the four edges and the applied displacements for the first group while figure no 10 shows the boundary conditions at the four edges and the applied displacements for the second group.

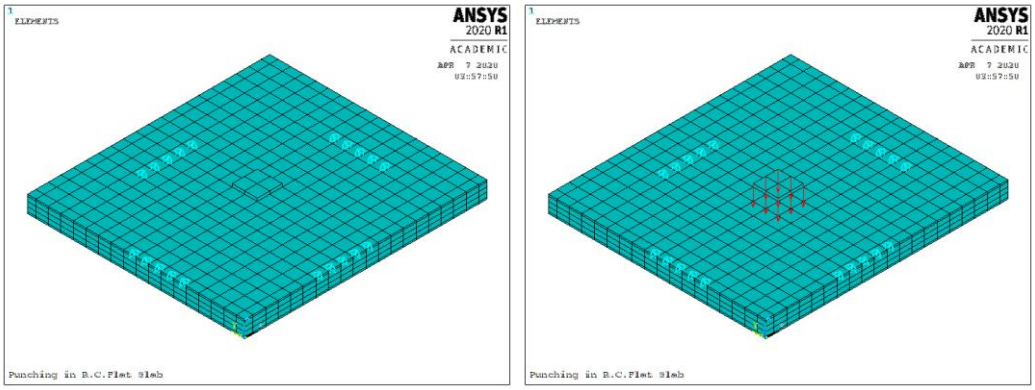

Figure no 9: Restraints and applied displacement for first group

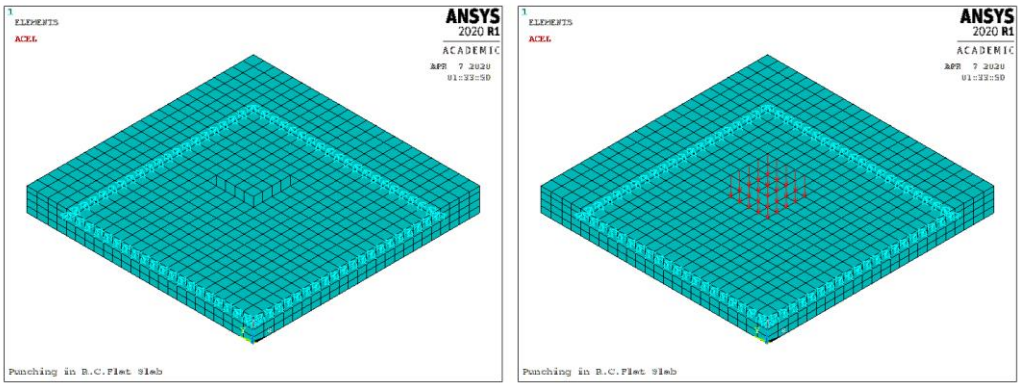

Figure no 10: Restraints and applied displacement for second group

Nonlinear analysis

The automatic time stepping was used to control the non-linear solution because of non-linear nature of considered problem. The full Newton-Raphson method (Bath, 1996) was activated to solve the non-linear equations. Residual force convergence criterion has been applied with reasonable tolerance to control the convergence of the non-linear solution.

Bond behavior

The bond between reinforcing bars and concrete was assumed perfect in accordance with that slab failure mode does not involve bond failure. Therefore, this assumption used in analysis will not cause a significant error in the predicted deformed shape and failure load.

V. Results

Table no 4 lists the results of all specimens. Figures no 11 and 12 showthe ultimate loads for both numerical and experimental work forgroup 1 and group 2, respectively. Figures no 13 and 14show the central deflections at ultimate loads for both numerical and experimental work forgroup 1 and group 2, respectively.

Table no 4: Ultimate load and central deflection (numerical versus experimental)

Group	Specimen	Experimental results [1,8]		Numerical Results		Numerical/Experimental	
		Max. load (KN)	Deflection (mm)	Max. load (KN)	Deflection (mm)	Load	Deflection
1	NN	670.4	16.7	675.64	16.67	1.008	0.998
	LA	552.0	10.6	556.63	11.28	1.008	1.064
	LD	626.3	15.2	605.96	14.80	0.968	0.974
2	Slab-I	8.0	0.32	8.60	0.34	1.075	1.063
	Slab-Ø6	34.5	6.2	34.77	6.0	1.008	0.968
	DP-2.0	25.0	4.5	26.30	4.25	1.052	0.944

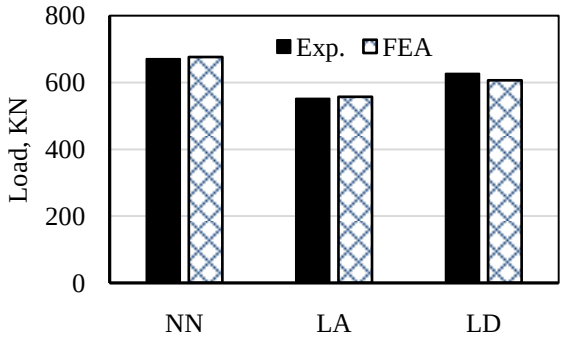

Figure no 11: Ultimate load -group 1 (FEA vs experiments)

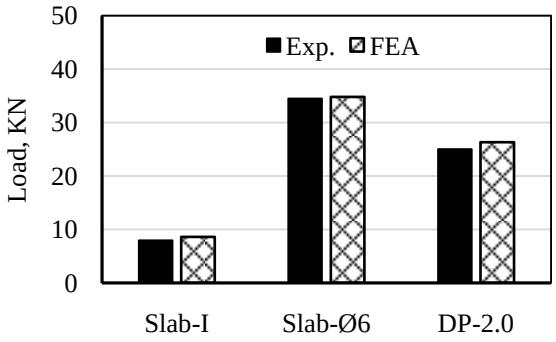

Figure no 12: Ultimate load - group 2 (FEA vs experiments)

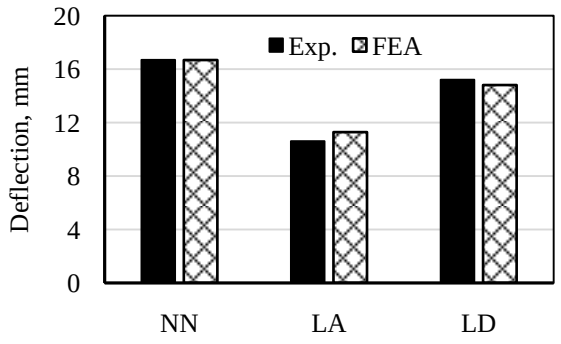

Figure no 13: Central deflection - group 1 (FEA versus experiments)

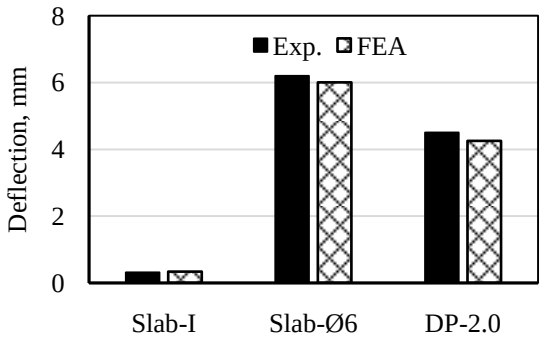

Figure no 14: Central deflection - group 2 (FEA versus experiments)

Figures no 15 to 20 show the numerical and experimental load-deflection responses at centers of the considered six slabs. The numerical results showed good agreement with experimental measurements.The variation between the numerical and experimental results were about 8% for failure loads and 7% for maximum deflections. Therefore, the proposed models gave realistic estimations for failure loads and displacements.

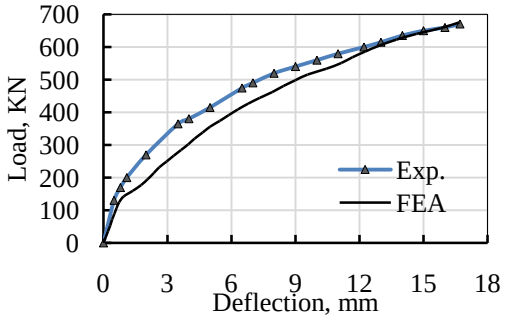

Figure no 15: Load-Deflection response, NN slab

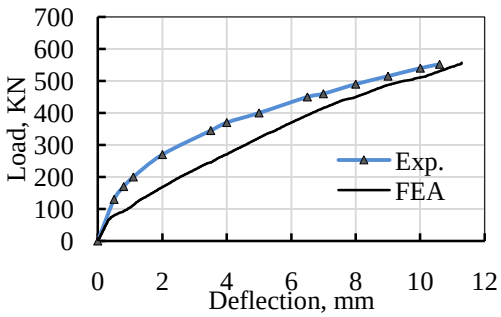

Figure no 16: Load-Deflection response, LA slab

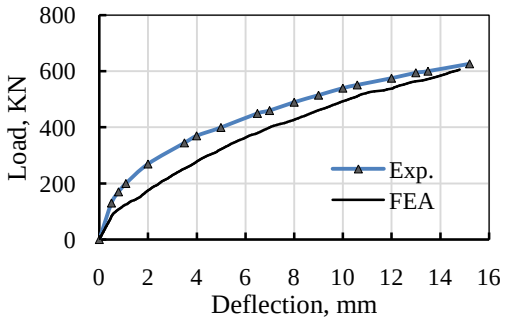

Figure no 17: Load-Deflection response, LD slab

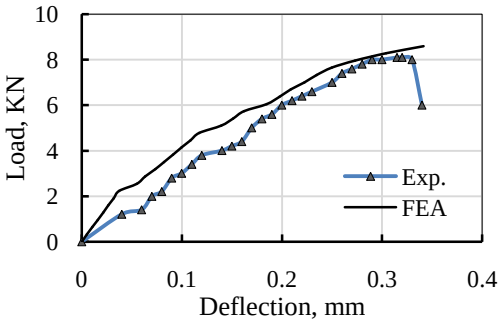

Figure no 18: Load-Deflection response, Slab-I

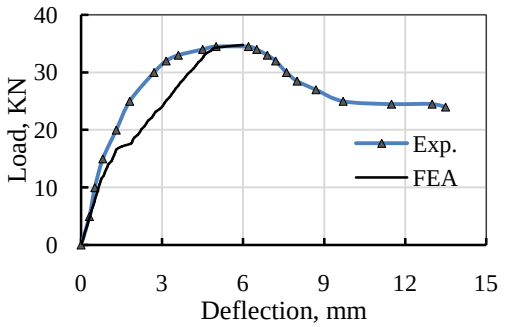

Figure no 19: Load-Deflection response, Slab-Ø6

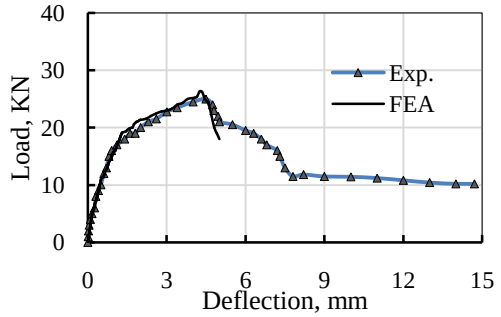

Figure no 20: Load-Deflection response, DP-2.0 slab

Figure no 21 shows comparisons between the numerical and experimental failure patternsfor slabs LA and LD.Figure no 22 shows thefailure patternsfor slab DP-2.0. The numerical results were matched well the experimental behavior.

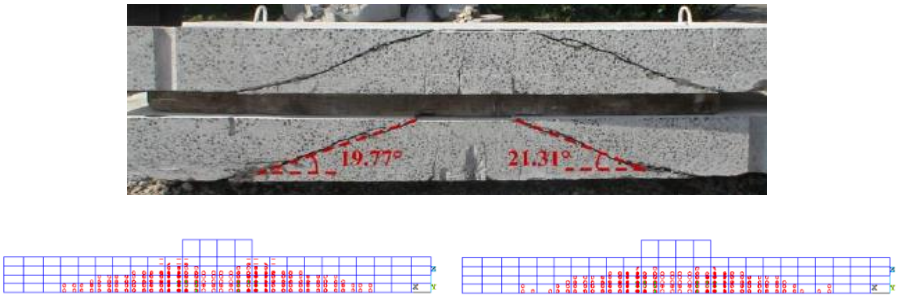

Figure no 21: Failure patterns for LA and LD slabs for both experimental and FEmodel

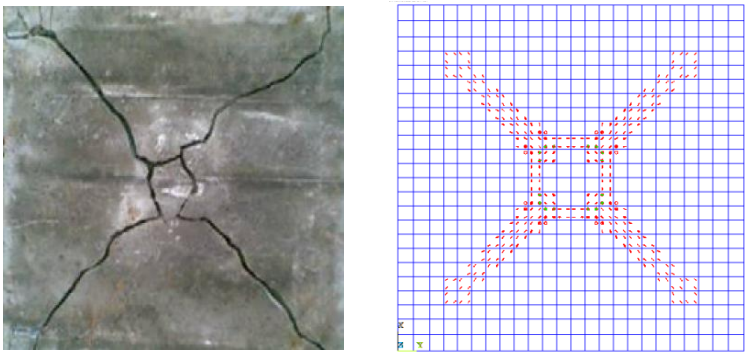

Figure no 22: Failure pattern for DP-2.0 slab for both experimental and FE model

VI. Conclusion

In this paper, finite element model was presented by using finite element analysis software (ANSYS V.2020.R1)to predict the punching shear response and strength of different types of slabs as normalweight reinforced concrete slabs, lightweight reinforced concrete slabs, cementitious slabs reinforced with regular grid of steel bars or with ferrocement layer and cementitious slabs without reinforcement. Three dimensional nonlinear FEA was conducted for six concrete slabs. The developed finite element models were based on and compared with the experimental programs of (Youm et al., 2014) and (Ibrahim, 2011). The predicted failure loads, central deflections at ultimate loads, deformed shapes and failure patterns were matched well with the experimental results.The differences between the numerical and experimental results were about 8% for failure loads and 7% for maximum deflections. The non-linear finite element analysis is robust tool for analyzing the behavior of punching shear response of different types of cementitious and concrete slabs. The developed finite element models could serve as a good tool for predicting the punching shear resistance for mentioned types of slabs and saved the high cost of experiments. Further exploring of the punching shear behavior and various parameters that affect the punching shear strength is now ready to be done numerically for large number of cases.

References

[1]. K. S. Youm, Jung J. Kim, J. Moon. Punching shear failure of slab with lightweight aggregate concrete (LWAC) and low reinforcement ratio. Construction and Building Materials. 2014; 65: 92–102.

[2]. Higashiyama, H., Mizukoshi, M. and Matsui, S. Punching shear strength of RC slabs using lightweight concrete. Challenges, Opportunities and Solutions in Structural Engineering and Construction – Ghafoori (ed.). 2010; 111-117.

[3]. Thai X. Dam, James K. Wight. Flexurally-triggered punching shear failure of reinforced concrete slab–column connections reinforced with headed shear studs arranged in orthogonal and radial layouts. Engineering Structures. 2016; 110: 258–268.

[4]. K. Venkateswarlu, V. Bhaskar Desai. Study of Concrete Modified with Artificial Cold Bonded Pelletized Light Weight Silica Fume Aggregates, IOSR Journal of Mechanical and Civil Engineering. 2018; Vol. 15, Issue 4: PP 51-60.

[5]. A. I. Tamboli, Atul, Harish Kasera, VivekMangal, AkritiZutshi, Ashwintyagi. Effective Internal Curing Using Light Weight Aggregates. IOSR Journal of Mechanical and Civil Engineering. 2016; Vol. 13, Issue 2: PP 49-52.

[6]. Naaman, A.E.Ferrocement and laminated cementitious composites. Cement & Concrete Composites. 2000; 22: 477-478.

[7]. Ibrahim, H. M. Experimental investigation of ultimate capacity of wired mesh-reinforced cementitious slabs. Constr Build Mater. 2011;25: 251-259.

[8]. Mashrei, M.A. Predicting punching shear strength of ferrocement slabs using back-propagation neural network. Thi_Qar U J Eng Sci. 2012; 3(2):85-102.

[9]. Mansur, M.A., Ahmad, I., and Paramasivam, P. Punching shear strength of simply supported ferrocement slabs. J. Mater. Civ. Eng –ASCE. 2001; 13(6): 418-426.

[10]. Paramasivam, P. and Tan, K. Punching shear strength of ferrocement slabs. ACI Struct J. 1993; 90(3): 294-301.

[11]. ANSYS (2009). ANSYS User's Manual. ANSYS, Inc., Southpointe, Canonsburg, PA, USA.

[12]. Taha A. El-Sayed, Abeer M. Erfan. Improving shear strength of beams using ferrocement composite. Construction and Building Materials; 2018, 172: 608–617.

[13]. Khan, H.U., Rafique, M.N., Karam, S., Ahmad, K. and Bashir A. Identification of shear cracks in reinforced beams using finite element method (ANSYS). Pakistan J Sci. 2014; 66(1): 50-55

[14]. Bathe, K.J. (1996). Finite Element Procedures. Prentice-Hall, Inc.

Hany A. Dahish,etal. "Finite Element Modeling of Lightweight Concrete Slabs with Expanded Metal Mesh." *IOSR Journal of Mechanical and Civil Engineering (IOSR-JMCE)*, 17(2), 2020, pp. 35-43.